Supporting Information

Salt Nanoconfinement in Zirconium-Based Metal-Organic Frameworks Leads to Pore-Size and Loading-Dependent Ionic Conductivity Enhancement

Sorout Shalini,[a] Thomas P. Vaid,[a] and Adam J. Matzger*[a,b]

[a] Department of Chemistry, University of Michigan, 930 North University Avenue, Ann Arbor, MI 48109, USA
[b] Department of Macromolecular Science and Engineering, University of Michigan, Ann Arbor, MI 48019, USA

*To whom correspondence should be addressed. Email address: matzger@umich.edu

Table of contents.

SI 1. Experimental Methods

UiO-66, UiO-67 and PCN-56 were synthesized using methods previously reported.[1,2] The dimethyl version of the terphenyl linker was used to make PCN-56 because the non-methylated version, UiO-68, is not reliably synthesized in crystalline form. Prior to salt loading, the MOFs were thoroughly washed with dimethylformamide (DMF) three times to remove unreacted starting compounds. DMF was then exchanged with ethanol for one day, during which ethanol was replenished thrice. Finally, the MOFs were activated by exposure to a dynamic vacuum (~10^{-2} Torr) at 120 °C for 18 hours.

[NEt_4][TFSI] preparation: [NEt_4][Br] (2.10 g, 10.0 mmol) was dissolved in 30 mL of water. LiTFSI (3.00 g, 10.5 mmol) was dissolved in 20 mL of water. The LiTFSI solution was slowly added to the [NEt_4][Br] solution, with stirring. A white precipitate formed immediately. The white solid was isolated by filtration and washed with water. The solid was air-dried for 16 h and then dried under vacuum and stored in a dry box. Yield: 3.343 g (81%). The PXRD pattern matched the reported pattern.[3]

The MOF-salt composites were prepared via melt loading where the MOF and salt were ground together and then heated at 130 °C for 12 h.

PXRD data were collected on a PANalytical Empyrean diffractometer in Bragg–Brentano geometry using Cu-Kα radiation (1.54187 Å), operating at 45 kV and 40 mA. The incident beam was equipped with a Bragg-BrentanoHD X-ray optic using fixed slits/soller slits. The detector was a silicon-based linear position sensitive X'Celerator Scientific operating in 1-D scanning mode. The samples were finely ground to minimize preferred orientation and packed in the depression of a glass slide and the data were collected from 4 to 50° 2θ with a step size of 0.008°.

Nitrogen sorption isotherms were measured on a NOVA e-Series 4200 surface area analyzer (Quantachrome Instruments). N_2 (99.999%) was purchased from Cryogenic Gases and used as received. Sorption isotherms were analyzed by NOVAwin software. For each N_2 measurement, a glass sample cell was charged with ~40 mg sample and analyzed at 77 K. The results are shown in figure S1.

Cyclic DSC experiments were carried out on TA Instrument Q20 differential scanning calorimeter. Precisely weighed samples were placed in Tzero™ hermetic aluminum pans and heated from 30 to 130 °C at a heating rate of 10 °C/min under nitrogen atmosphere, held at 130 °C for 5 minutes, and cooled back to 30 °C. For the subsequent cycles the hold time was half an hour. The experiment was run until the melt endotherm for the salt disappeared.

The Interface 1010E potentiostat (Gamry instruments) was used to carry out the impedance measurement. The impedance spectra were recorded by applying a range of frequency from 1 MHz to 100 mHz with an amplitude of 10 mV. The measurements were done at room

temperature, 40, 60, 70, 80, and 90 °C under ambient atmosphere. To ensure that the materials do not adsorb moisture, the physical mixture of MOF and salt were ground in a glove box, heated in a glass vial sealed under nitrogen. The sample was then pressed into a pellet using a 5mm evacuable pellet die and quickly loaded into the sample cell.

SI 2. N_2 sorption isotherms for UiO-66, UiO-67, and PCN-56

N_2 sorption isotherms were measured on all MOFs prior to salt loading to ensure their phase purity and structural integrity. BET surface area was found to be in close agreement with the reported surface area.

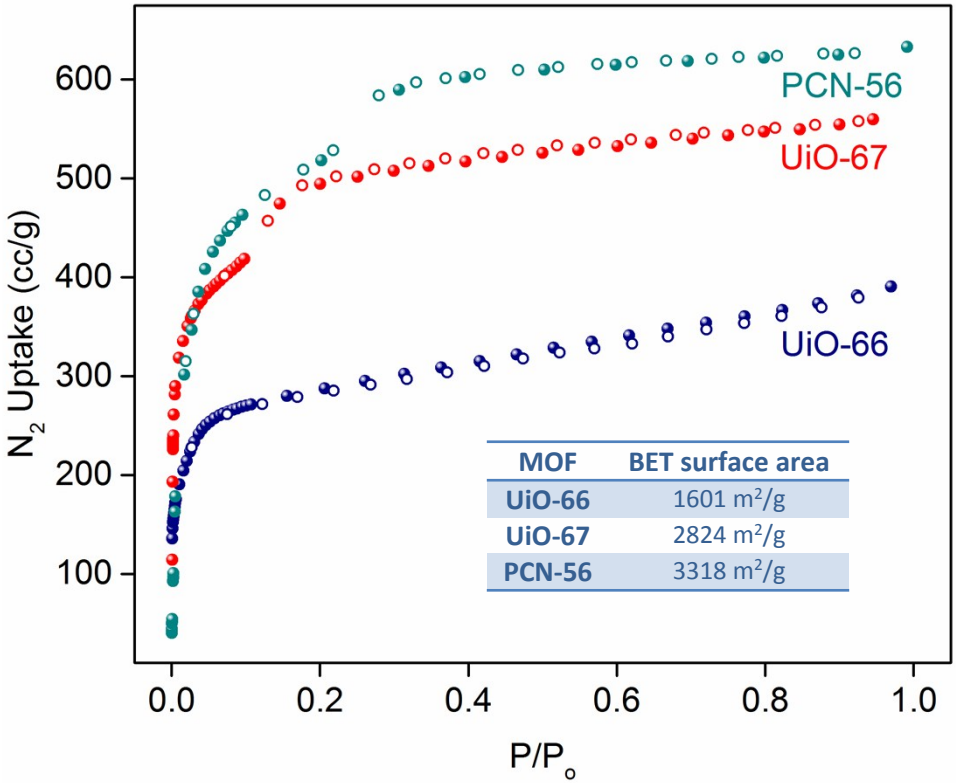

Figure S1. N_2 sorption isotherms of UiO-66, UiO-67, and PCN-56 where the filled circles show adsorption and hollow circles show desorption at 77K. The inset shows the BET surface area for all three MOFs calculated from the isotherms.

SI 3. Simulated and experimental PXRDs of MOFs

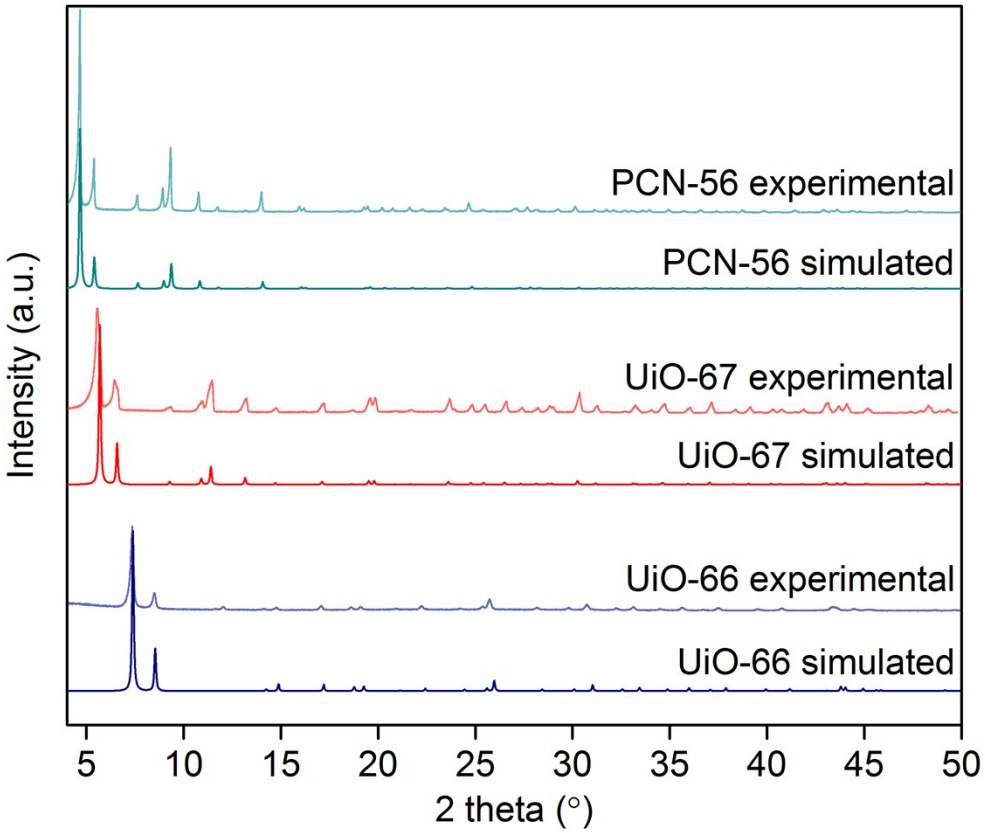

Figure S2. Comparison of experimental and simulated powder diffraction patterns of UiO-66, UiO-67, and PCN-56 confirming their bulk phase purity.

SI 4. Weight % loading tested for MOFs

Table S1. Theoretical number of [NEt_4][TFSI] ion pairs that fit in each pore in the three MOFs.

MOF	(1/4) unit cell volume (Å^3)	void volume (Å^3)	# ion pairs (1 O_h and 2 T_d pores)	ion pairs in O_h pore	ion pairs in T_d pore
UiO-66	2308	1110	2.5	1.3	0.6
UiO-67	4972	3257	7.4	3.7	1.8
PCN-56	8662	6306	14.3	7.1	3.6

For Table 1 above, the volume of a single [NEt_4][TFSI] ion pair was calculated to be 441 Å^3 using the crystallographic density of 1.544 g·cm^{-3} and a formula mass of 410.39 g·mol^{-1}. Unit cell void volumes were determined with Mercury, and the approximation was made that the volume of the octahedral pores is twice the volume of the tetrahedral pores (and there are two tetrahedral pores for each octahedral pore in the structure of the MOFs).

Table S2. Loading of salt in MOFs at different compositions.

Wt % of salt	Complete loading of salt in MOF		
	UiO-66	UiO-67	PCN-56
33.3	Yes	Yes	Yes
38.4	Yes	Yes	Yes
42.8	No	Yes	Yes
46.6	No	Yes	Yes
50.0	N/A	No	Yes
53.2*	N/A	No	No
57.1	N/A	N/A	No

*The corresponding loading for UiO-67 is 52.9%

SI 5. Cyclic DSC of MOF-salt composites

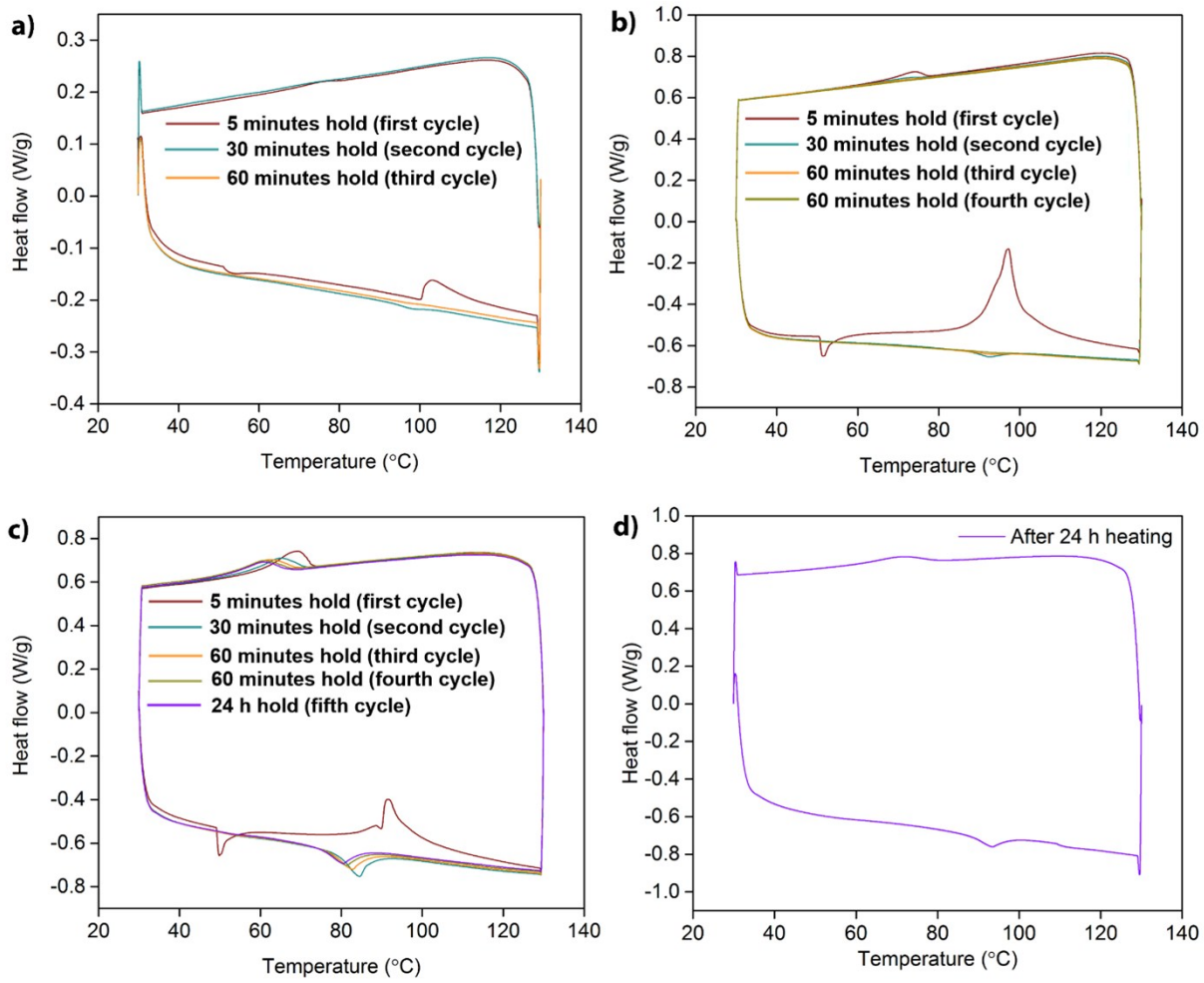

Figure S3. DSC traces of UiO-66/[NEt_4][TFSI] system; a) UiO-66 33.3 wt% [NEt_4][TFSI], b) UiO-66 38.4 wt% [NEt_4][TFSI], c) UiO-66 42.8 wt% [NEt_4][TFSI], and d) UiO-66 46.6 wt% [NEt_4][TFSI]. The disappearance of endotherm supports the complete loading of salt in 35 minutes for systems with 33.3 wt% and 38.4 wt% [NEt_4][TFSI] while the salt does not load completely even after 24 h for 42.8 wt% and 46.6 wt% [NEt_4][TFSI] systems suggesting the maximum loading of salt in UiO-66 to be 38.4 wt%.

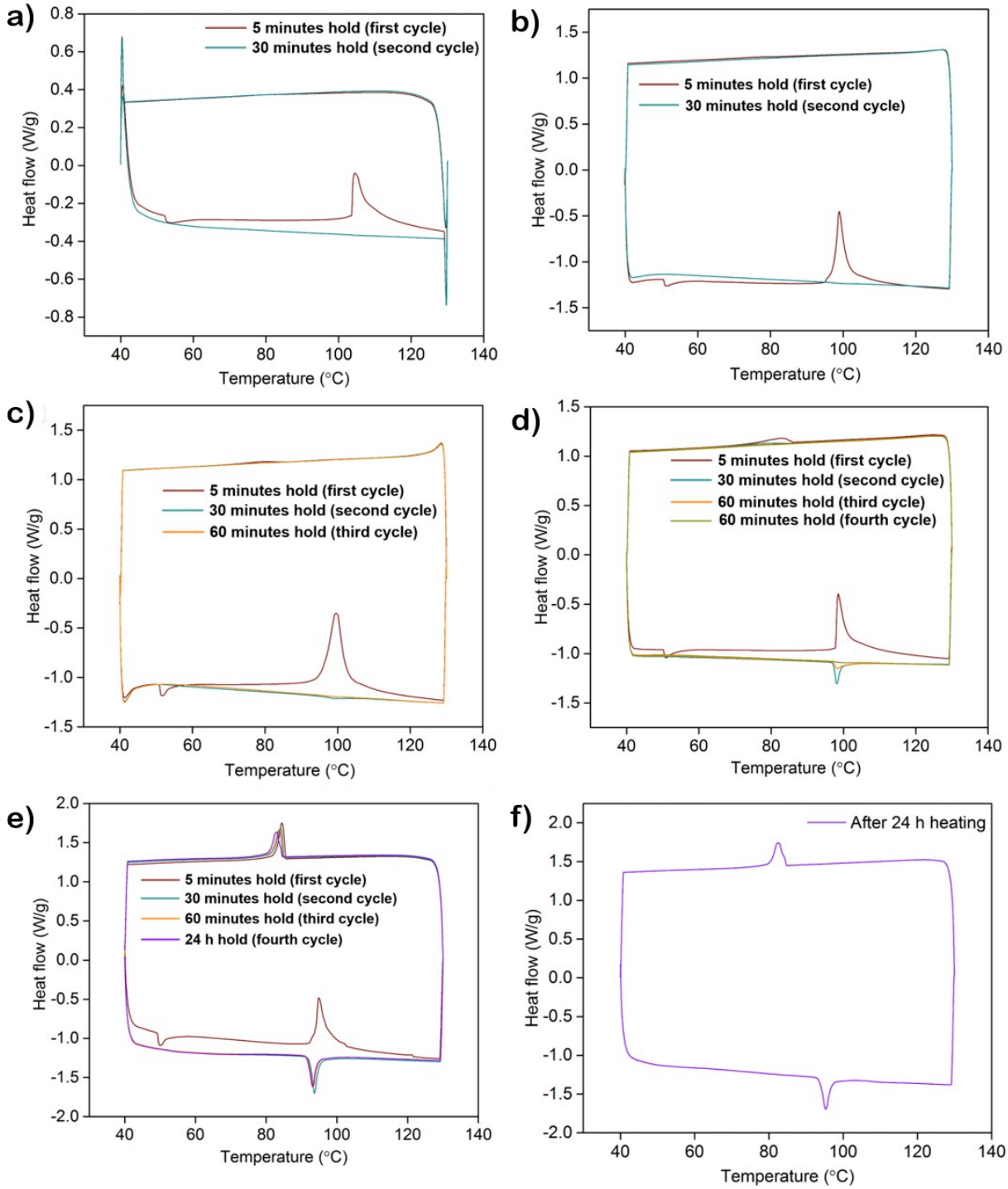

Figure S4. DSC traces of UiO-67/[NEt_4][TFSI] system; a) UiO-67 33.3 wt% [NEt_4][TFSI], b) 38.4 % [NEt_4][TFSI], c) UiO-67 42.8 wt% [NEt_4][TFSI], d) UiO-67 46.6 wt% [NEt_4][TFSI], e) 50.0 % [NEt_4][TFSI and f) UiO-67 52.9 wt% [NEt_4][TFSI]. The disappearance of endotherm supports the complete loading of salt in 5 minutes for system with 33.3 wt% and 38.4 wt% [NEt_4][TFSI], 35 minutes for system with 42.8 wt% [NEt_4][TFSI], 95 minutes for system with 46.6 wt% [NEt_4][TFSI] while the salt does not load completely even after 24 h for 50 wt % and 52.9 wt% [NEt_4][TFSI] system suggesting the maximum loading of salt in UiO-67 to be 46.6 wt%.

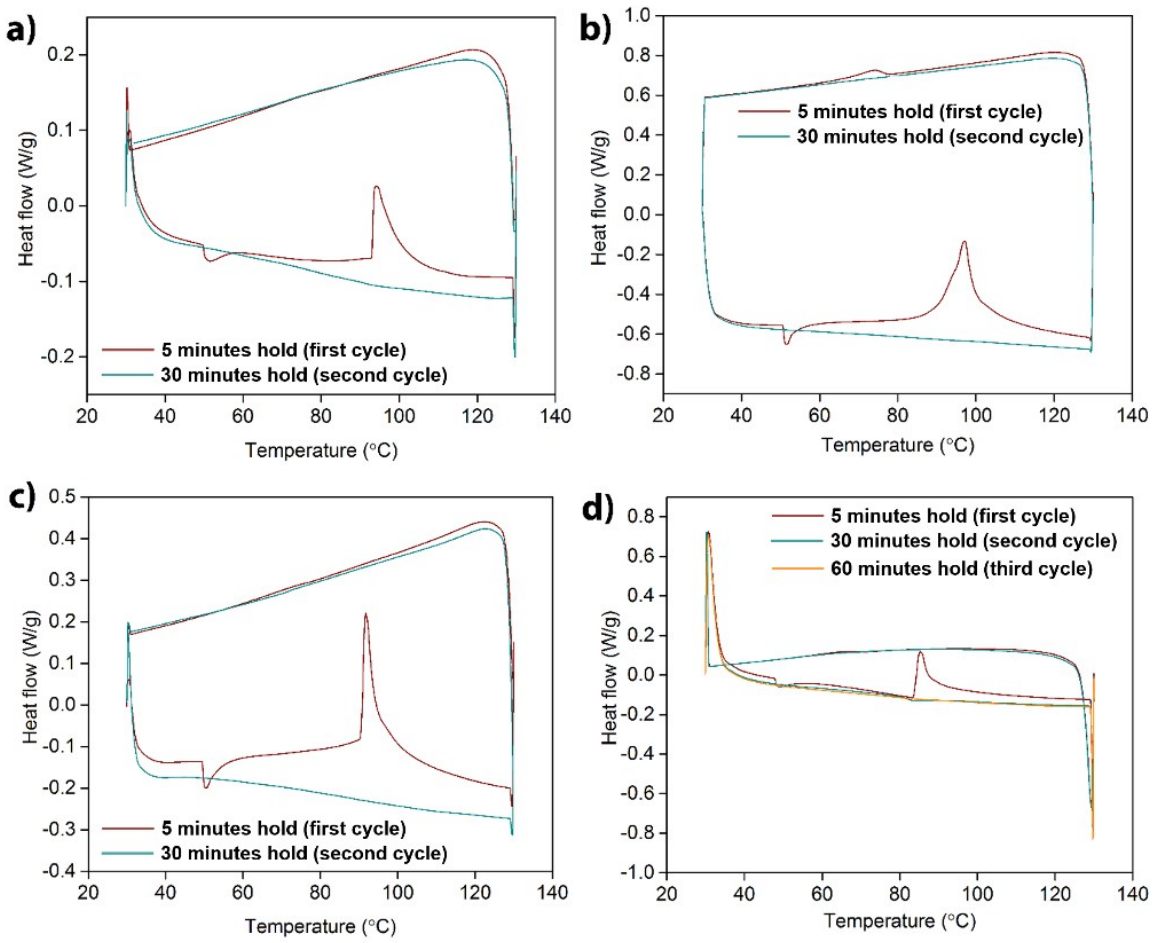

Figure S5. DSC traces of PCN-56/[NEt_4][TFSI] system; a) PCN-56 33.3 wt% [NEt_4][TFSI], b) PCN-56 38.4 wt% [NEt_4][TFSI], c) PCN-56 42.8 wt% [NEt_4][TFSI], and d) PCN-56 46.6 wt% [NEt_4][TFSI]. The disappearance of endotherm supports the complete loading of salt in 5 minutes for systems with 33.3 wt%, 38.4 wt%, and 42.8 wt% [NEt_4][TFSI], and 35 minutes for system with 46.6 wt% [NEt_4][TFSI].

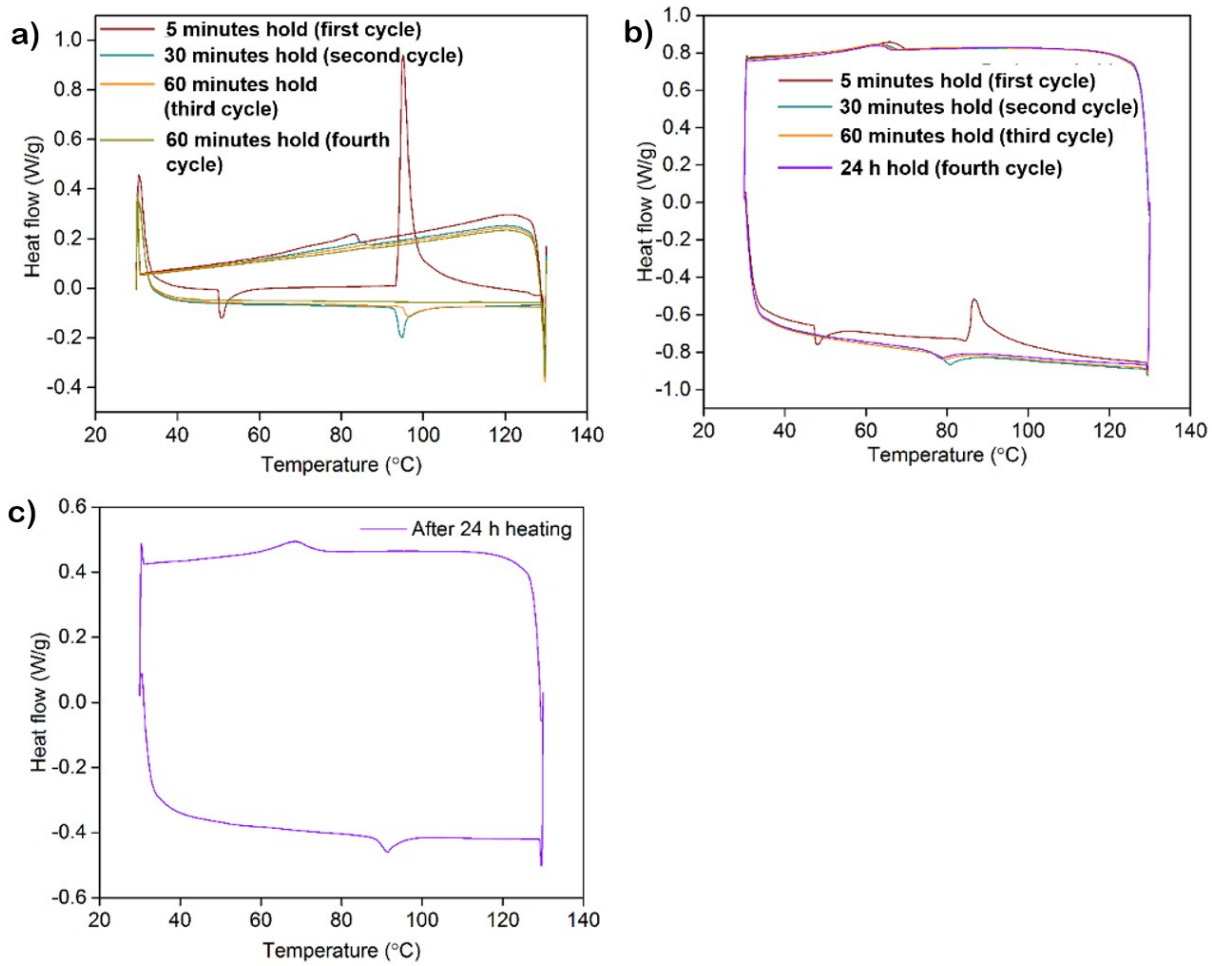

Figure S6. DSC traces of PCN-56/[NEt_4][TFSI] system; a) PCN-56 50 wt% [NEt_4][TFSI], b) PCN-56 53.2 wt% [NEt_4][TFSI], and c) PCN-56 57.08 wt% [NEt_4][TFSI] . The disappearance of endotherm supports the complete loading of salt in 95 minutes for system with 50 wt% [NEt_4][TFSI] while the salt does not load completely even after 24 h for 53.2 wt% and 57.08 wt% [NEt_4][TFSI] systems suggesting the maximum loading of salt in PCN-56 to be 50 wt%.

SI 6. PXRD of MOF-salt composites

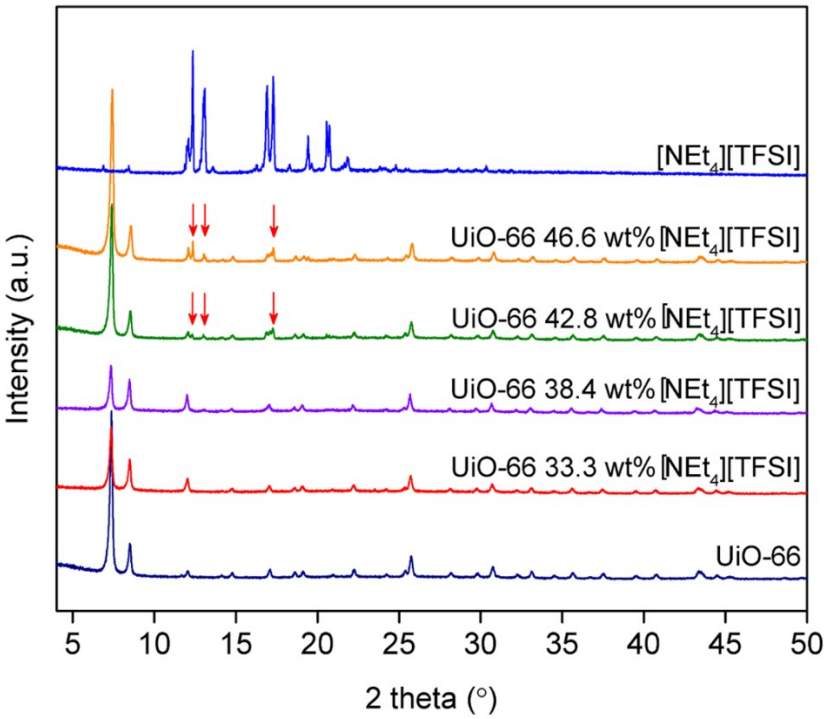

Figure S7. Powder diffraction patterns of UiO-66-salt composites. The red arrows show the diffraction peaks for salt implying the presence of salt outside the MOF.

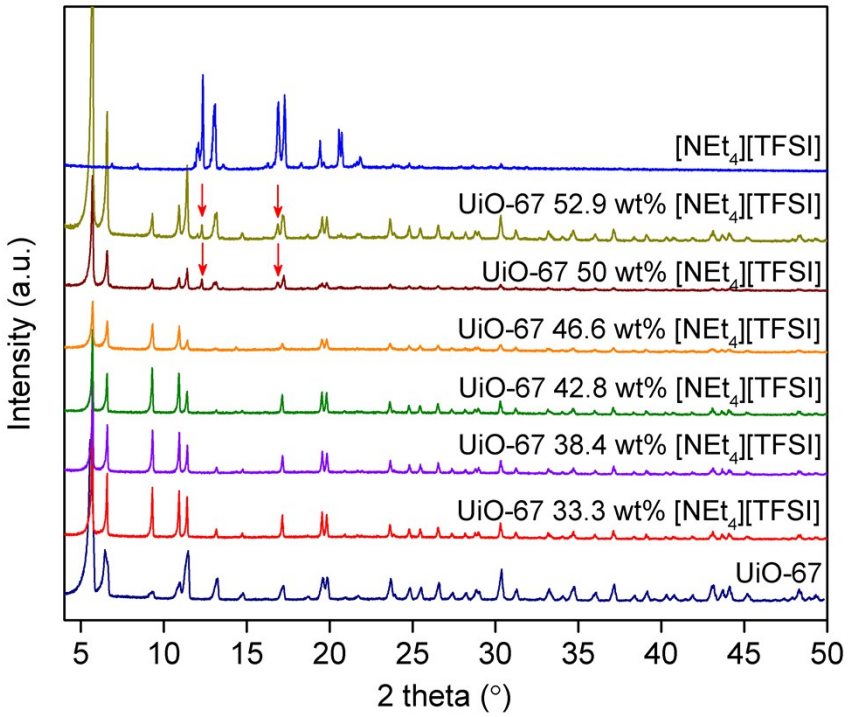

Figure S8. Powder diffraction patterns of UiO-67-salt composites. The red arrows show the diffraction peaks for salt implying the presence of salt outside the MOF.

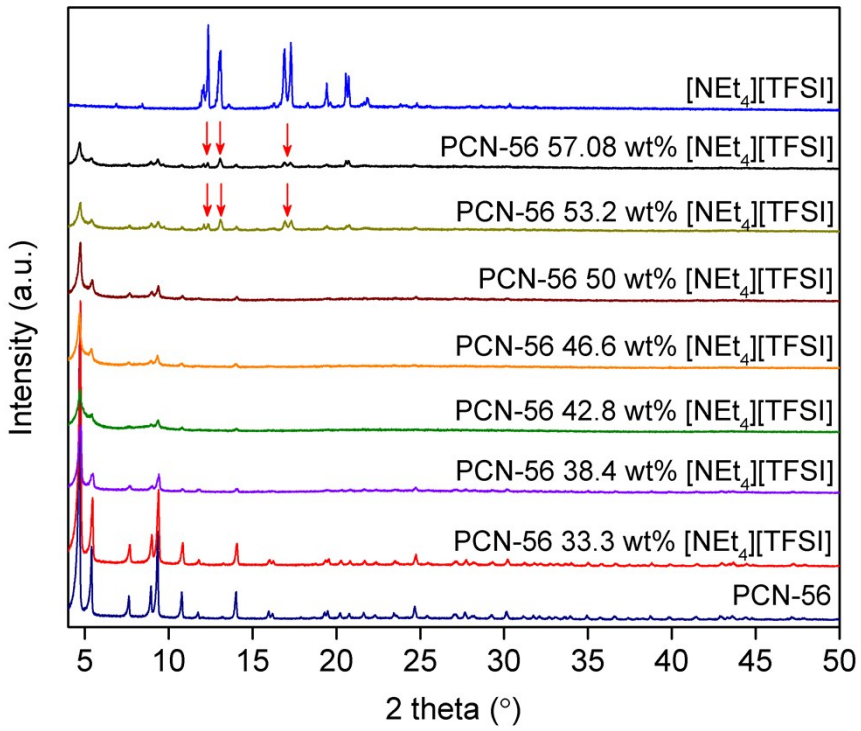

Figure S9. Powder diffraction patterns of PCN-56-salt composites. The red arrows show the diffraction peaks for salt implying the presence of salt outside the MOF.

SI 7. AC impedance spectroscopy of MOF-salt composites

The appropriate mass ratio of MOF and [NEt_4][TFSI] were ground together, heated to 130 °C for 12 h, and pressed into a 0.50 cm diameter pellet in a die at 3500 bar pressure. The pelletized samples were loaded in an MTI EQ-STC test cell in a laboratory oven for temperature control. At each temperature the semicircle of the Nyquist plot was extrapolated to the baseline to obtain the real impedance of the sample at that temperature. That value was used as the resistance of the sample, which was converted to resistivity (and conductivity) using the known area of the circular pellet and its measured thickness.

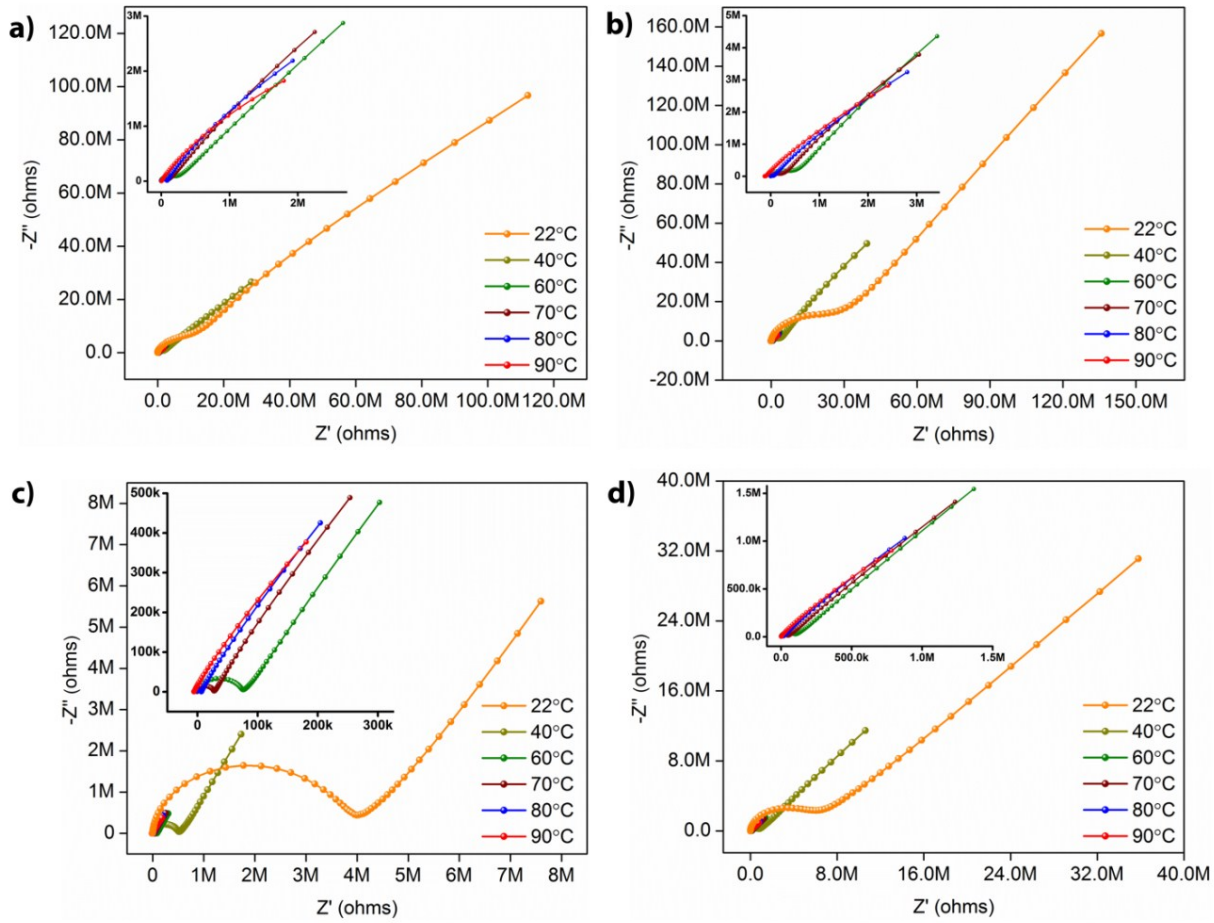

Figure S10. Nyquist plots for a) UiO-66 33.3 wt% [NEt_4][TFSI], b) UiO-66 38.4 wt%, [NEt_4][TFSI], c) UiO-66 42.8 wt% [NEt_4][TFSI], and d) UiO-66 46.6 wt% [NEt_4][TFSI] showing the variation of resistance with temperature.

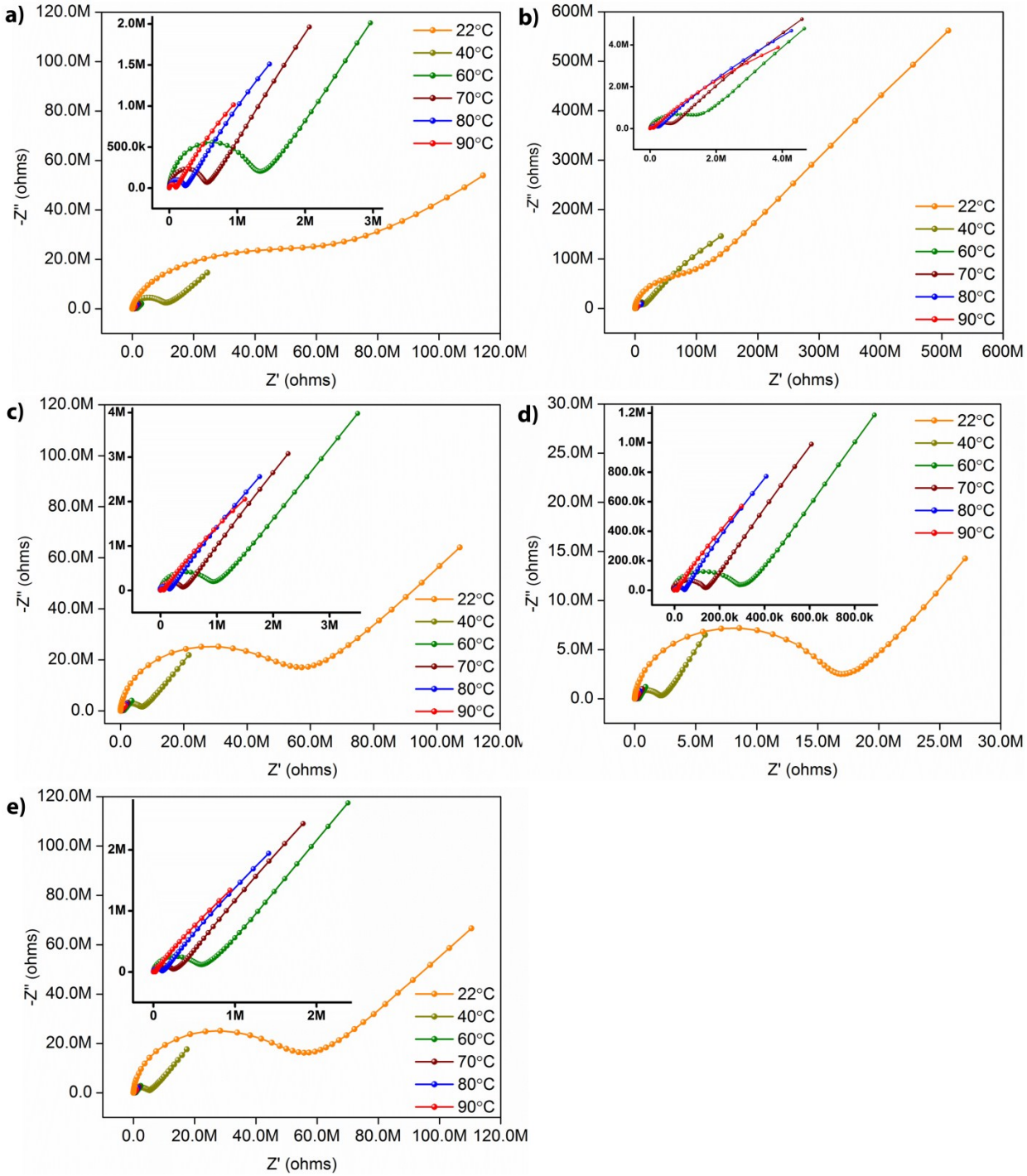

Figure S11. Nyquist plots for a) UiO-67 33.3 wt% [NEt_4][TFSI], b) UiO-67 38.4 wt%, [NEt_4][TFSI], c) UiO-67 46.6 wt% [NEt_4][TFSI], d) UiO-67 50 wt% [NEt_4][TFSI], and e) UiO-67 52.9 wt% [NEt_4][TFSI] showing the variation of resistance with temperature.

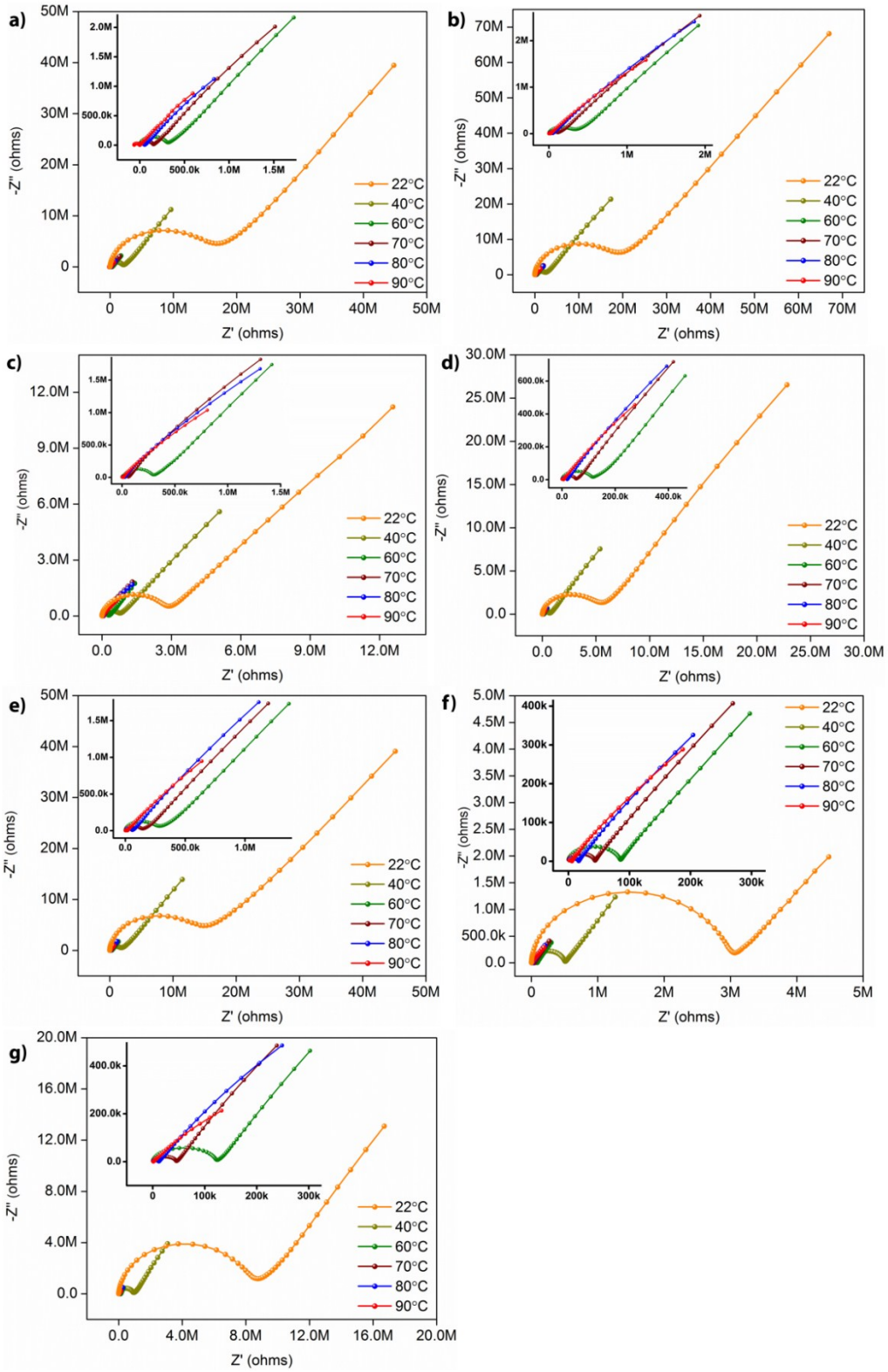

Figure S12. Nyquist plots for a) PCN-56 33.3 wt% [NEt_4][TFSI], b) PCN-56 38.4 wt%, [NEt_4][TFSI], c) PCN-56 42.8 wt% [NEt_4][TFSI], d) PCN-56 46.6 wt% [NEt_4][TFSI], e) PCN-56 50 wt% [NEt_4][TFSI], f) PCN-56 53.2 wt%, and g) PCN-56 57.08 [NEt_4][TFSI] showing the variation of resistance with temperature.

SI 8. Calculation of ionic conductivity and activation energy of MOF-salt composites

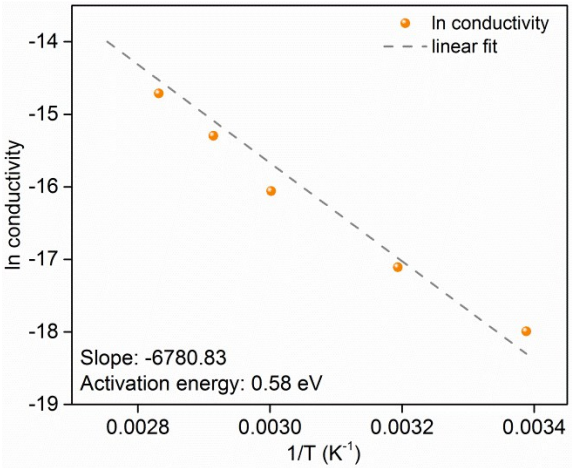

Figure S13. Logarithmic plot of conductivity vs. temperature for [NEt_4][TFSI] used to calculate the activation energy.

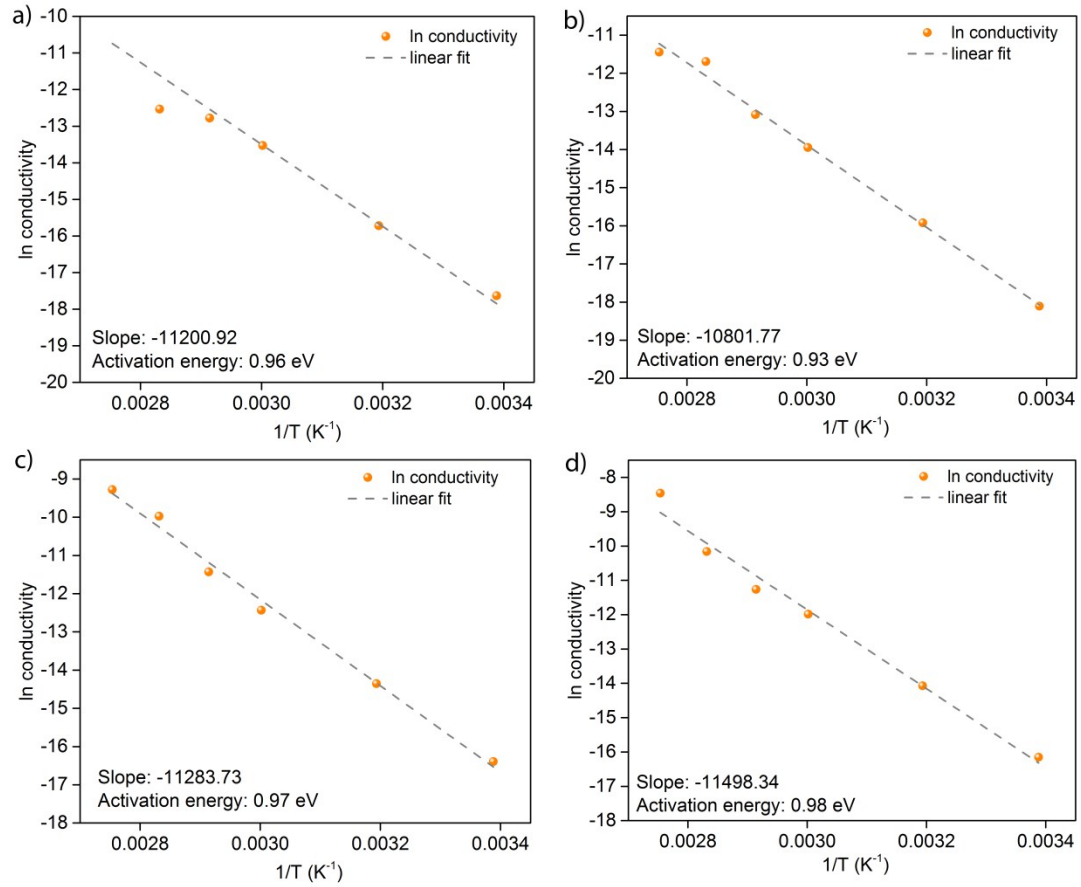

Figure S14. Logarithmic plot of conductivity vs. temperature for a) UiO-66 33.3 wt% [NEt_4][TFSI], b) UiO-66 38.4 wt%, [NEt_4][TFSI], c) UiO-66 42.8 wt% [NEt_4][TFSI], and d) UiO-66 46.6 wt% [NEt_4][TFSI] used to calculate the activation energy.

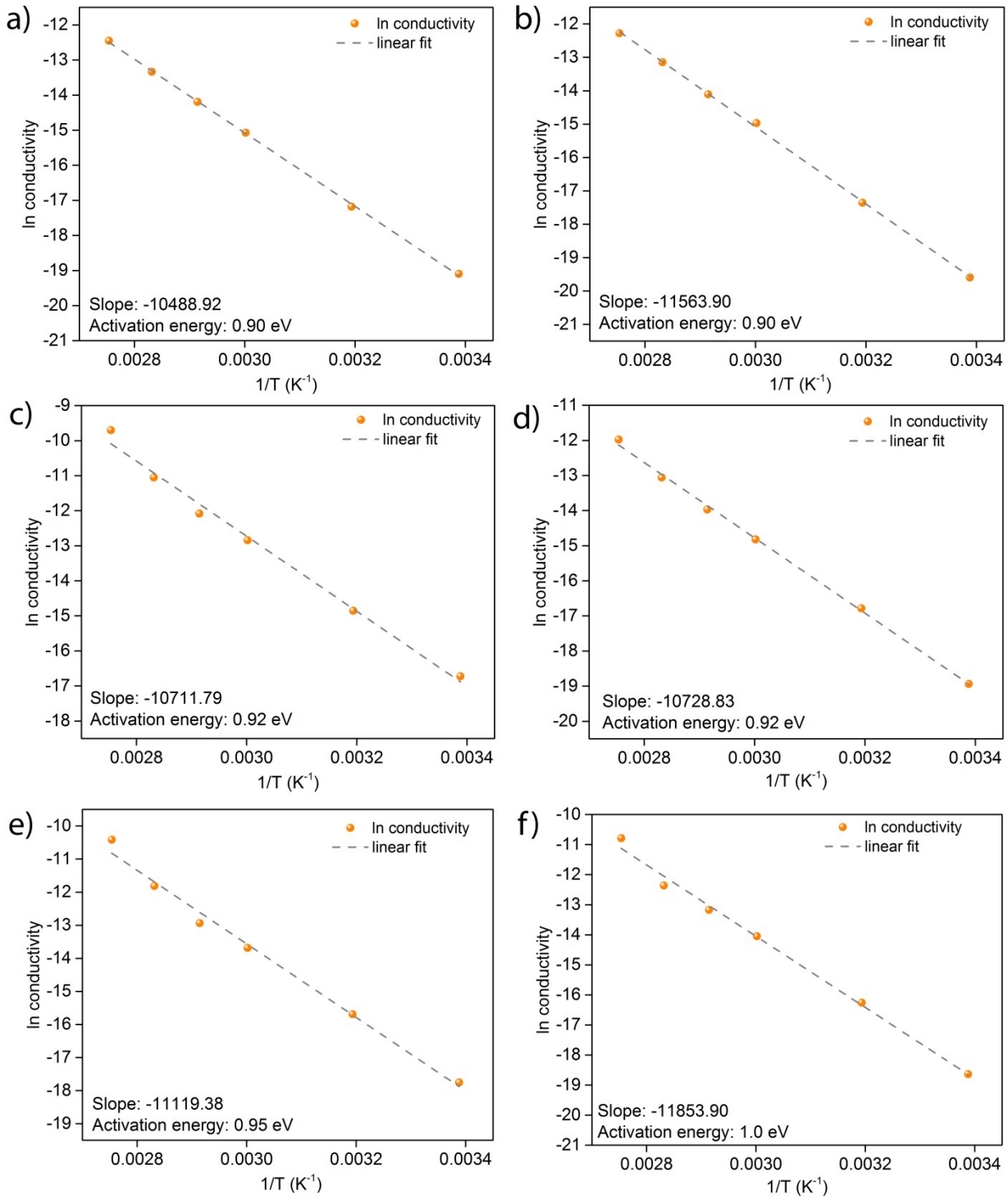

Figure S15. Logarithmic plot of conductivity vs. temperature for a) UiO-67 33.3 wt% [NEt_4][TFSI], b) UiO-67 38.4 wt%, [NEt_4][TFSI], c) UiO-67 42.8 wt% [NEt_4][TFSI], d) UiO-67 46.6 wt% [NEt_4][TFSI], e) UiO-67 50 wt% [NEt_4][TFSI], and f) UiO-67 52.9 wt% [NEt_4][TFSI] used to calculate the activation energy.

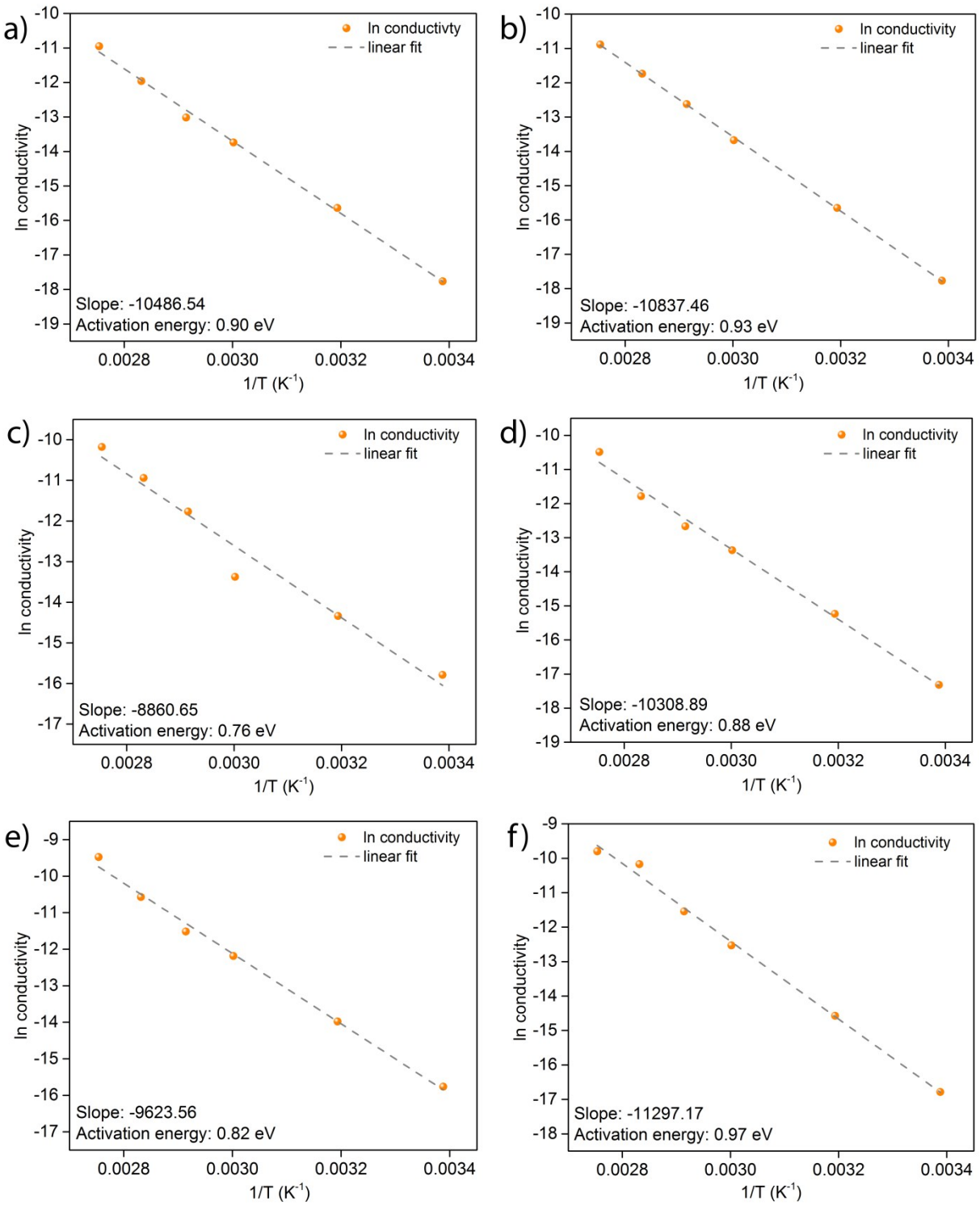

Figure S16. Logarithmic plot of conductivity vs. temperature for a) PCN-56 33.3 wt% [NEt_4][TFSI], b) PCN-56 38.4 wt%, [NEt_4][TFSI], c) PCN-56 42.8 wt% [NEt_4][TFSI], d) PCN-56 50 wt% [NEt_4][TFSI], e) PCN-56 53.2 wt%, and f) PCN-56 57.08 [NEt_4][TFSI] used to calculate the activation energy

Table S3. Calculation of ionic conductivity and activation energy of [NEt_4][TFSI]

Temperature (°C)	Resistance (Ohms)	Thickness (cm)	Area (cm^2)	Conductivity (S/cm)	1/T (K^{-1})	ln (Conductivity)	Activation Energy (eV)
22	14500000	0.043	0.193	1.54E-08	0.003388	-17.54765678	0.58
40	6000000	0.043	0.193	3.71E-08	0.003193	-16.6652676	
60	2100000	0.043	0.193	1.06E-07	0.003002	-15.61544547	
70	978600	0.043	0.193	2.28E-07	0.002914	-15.29536833	
80	546800	0.043	0.193	4.07E-07	0.002832	-14.71332846	
90	149200	0.043	0.193	1.49E-06	0.002754	-13.41453304	

Table S4. Calculation of ionic conductivity and activation energy of UiO-66 33.3 wt% [NEt_4][TFSI].

Temperature (°C)	Resistance (Ohms)	Thickness (cm)	Area (cm^2)	Conductivity (S/cm)	1/T (K^{-1})	ln (Conductivity)	Activation Energy (eV)
22	13758645	0.05842	0.193	2.20E-08	0.003388	-17.6322098	0.96
40	2034048	0.05842	0.193	1.49E-07	0.003193	-15.72057035	
60	227400	0.05842	0.193	1.33E-06	0.003002	-13.52949775	
70	107100	0.05842	0.193	2.83E-06	0.002914	-12.77655015	
80	83870	0.05842	0.193	3.61E-06	0.002832	-12.53205515	
90	5117	0.05842	0.193	5.92E-05	0.002754	-9.735355501	

Table S5. Calculation of ionic conductivity and activation energy of UiO-66 38.4 wt% [NEt_4][TFSI].

Temperature (°C)	Resistance (Ohms)	Thickness (cm)	Area (cm^2)	Conductivity (S/cm)	1/T (K^{-1})	ln (Conductivity)	Activation Energy (eV)
22	30785235	0.08128	0.193	1.37E-08	0.003388	-18.10733595	0.93
40	3460695	0.08128	0.193	1.22E-07	0.003193	-15.9217702	
60	482352	0.08128	0.193	8.73E-07	0.003002	-13.95121962	
70	202800	0.08128	0.193	2.08E-06	0.002914	-13.08476576	
80	50360	0.08128	0.193	8.36E-06	0.002832	-11.69174269	
90	39290	0.08128	0.193	1.07E-05	0.002754	-11.44351552	

Table S6. Calculation of ionic conductivity and activation energy of UiO-66 42.2 wt% [NEt_4][TFSI].

Temperature (°C)	Resistance (Ohms)	Thickness (cm)	Area (cm^2)	Conductivity (S/cm)	1/T (K^{-1})	ln (Conductivity)	Activation Energy (eV)
22	3994000	0.05842	0.193	7.58E-08	0.003388	-16.39533568	0.97
40	518300	0.05842	0.193	5.84E-07	0.003193	-14.3533414	
60	75910	0.05842	0.193	3.99E-06	0.003002	-12.4323356	
70	27820	0.05842	0.193	1.09E-05	0.002914	-11.42854236	
80	6506	0.05842	0.193	4.65E-05	0.002832	-9.975511999	
90	3240	0.05842	0.193	9.34E-05	0.002754	-9.278360501	

Table S7. Calculation of ionic conductivity and activation energy of UiO-66 46.6 wt% $[NEt_4][TFSI]$.

Temperature (°C)	Resistance (Ohms)	Thickness (cm)	Area (cm^2)	Conductivity (S/cm)	1/T (K^{-1})	ln (Conductivity)	Activation Energy (eV)
22	6683619	0.12446	0.193	9.65E-08	0.003388	-16.15387598	0.98
40	834700	0.12446	0.193	7.73E-07	0.003193	-14.07353347	
60	103600	0.12446	0.193	6.22E-06	0.003002	-11.98699842	
70	50360	0.12446	0.193	1.28E-05	0.002914	-11.2656583	
80	16650	0.12446	0.193	3.87E-05	0.002832	-10.15887131	
90	3041	0.12446	0.193	2.12E-04	0.002754	-8.458647497	

Table S8. Calculation of ionic conductivity and activation energy of UiO-67 33.3 wt% $[NEt_4][TFSI]$.

Temperature (°C)	Resistance (Ohms)	Thickness (cm)	Area (cm^2)	Conductivity (S/cm)	1/T (K^{-1})	ln (Conductivity)	Activation Energy (eV)
22	75050343	0.07366	0.193	5.09E-09	0.003388	-19.09689996	0.90
40	11030000	0.07366	0.193	3.46E-08	0.003193	-17.17935967	
60	1342000	0.07366	0.193	2.84E-07	0.003002	-15.07290187	
70	556300	0.07366	0.193	6.86E-07	0.002914	-14.19229327	
80	235700	0.07366	0.193	1.62E-06	0.002832	-13.33354537	
90	97500	0.07366	0.193	3.91E-06	0.002754	-12.45083793	

Table S9. Calculation of ionic conductivity and activation energy of UiO-67 38.4 wt% $[NEt_4][TFSI]$.

Temperature (°C)	Resistance (Ohms)	Thickness (cm)	Area (cm^2)	Conductivity (S/cm)	1/T (K^{-1})	ln (Conductivity)	Activation Energy (eV)
22	148718535	0.0889	0.193	3.10E-09	0.003388	-19.5927441	0.99
40	15870404	0.0889	0.193	2.90E-08	0.003193	-17.3551446	
60	1464000	0.0889	0.193	3.15E-07	0.003002	-14.97186102	
70	618300	0.0889	0.193	7.45E-07	0.002914	-14.1099071	
80	236400	0.0889	0.193	1.95E-06	0.002832	-13.14845861	
90	99290	0.0889	0.193	4.64E-06	0.002754	-12.28097819	

Table S10. Calculation of ionic conductivity and activation energy of UiO-67 42.8 wt% $[NEt_4][TFSI]$.

Temperature (°C)	Resistance (Ohms)	Thickness (cm)	Area (cm^2)	Conductivity (S/cm)	1/T (K^{-1})	ln (Conductivity)	Activation Energy (eV)
22	9422000	0.09906	0.193	5.45E-08	0.003388	-16.7255224	0.92
40	1447000	0.09906	0.193	3.55E-07	0.003193	-14.85196747	
60	194000	0.09906	0.193	2.65E-06	0.003002	-12.8425779	
70	90450	0.09906	0.193	5.67E-06	0.002914	-12.07951695	
80	32270	0.09906	0.193	1.59E-05	0.002832	-11.04885775	
90	8382	0.09906	0.193	6.12E-05	0.002754	-9.70080629	

Table S11. Calculation of ionic conductivity and activation energy of UiO-67 46.6 wt% [NEt_4][TFSI].

Temperature (°C)	Resistance (Ohms)	Thickness (cm)	Area (cm^2)	Conductivity (S/cm)	1/T (K^{-1})	ln (Conductivity)	Activation Energy (eV)
22	57300000	0.06604	0.193	5.97E-09	0.003388	-18.93624075	0.92
40	6675000	0.06604	0.193	5.13E-08	0.003193	-16.78630933	
60	935000	0.06604	0.193	3.66E-07	0.003002	-14.82073138	
70	398500	0.06604	0.193	8.59E-07	0.002914	-13.96789235	
80	160400	0.06604	0.193	2.13E-06	0.002832	-13.05785554	
90	54460	0.06604	0.193	6.28E-06	0.002754	-11.97765134	

Table S12. Calculation of ionic conductivity and activation energy of UiO-67 50 wt% [NEt_4][TFSI].

Temperature (°C)	Resistance (Ohms)	Thickness (cm)	Area (cm^2)	Conductivity (S/cm)	1/T (K^{-1})	ln (Conductivity)	Activation Energy (eV)
22	16910000	0.0635	0.193	1.95E-08	0.003388	-17.755066	0.95
40	2151000	0.0635	0.193	1.53E-07	0.003193	-15.69309369	
60	288600	0.0635	0.193	1.14E-06	0.003002	-13.68444721	
70	136300	0.0635	0.193	2.41E-06	0.002914	-12.9342639	
80	44510	0.0635	0.193	7.39E-06	0.002832	-11.81511945	
90	10990	0.0635	0.193	2.99E-05	0.002754	-10.41639133	

Table S13. Calculation of ionic conductivity and activation energy of UiO-67 52.9 wt% [NEt_4][TFSI].

Temperature (°C)	Resistance (Ohms)	Thickness (cm)	Area (cm^2)	Conductivity (S/cm)	1/T (K^{-1})	ln (Conductivity)	Activation Energy (eV)
22	57350000	0.0889	0.193	8.03E-09	0.003388	-18.63986145	1.0
40	5298000	0.0889	0.193	8.69E-08	0.003193	-16.258018	
60	583500	0.0889	0.193	7.89E-07	0.003002	-14.05197778	
70	243200	0.0889	0.193	1.89E-06	0.002914	-13.17681748	
80	107800	0.0889	0.193	4.27E-06	0.002832	-12.36321098	
90	22270	0.0889	0.193	2.07E-05	0.002754	-10.78617381	

Table S14. Calculation of ionic conductivity and activation energy of PCN-56 33.3 wt% [NEt_4][TFSI].

Temperature (°C)	Resistance (Ohms)	Thickness (cm)	Area (cm^2)	Conductivity (S/cm)	1/T (K^{-1})	ln (Conductivity)	Activation Energy (eV)
22	17770000	0.06604	0.193	1.93E-08	0.003388	-17.76545177	0.90
40	2123000	0.06604	0.193	1.61E-07	0.003193	-15.64077031	
60	317000	0.06604	0.193	1.08E-06	0.003002	-13.73908662	
70	153900	0.06604	0.193	2.22E-06	0.002914	-13.01648789	
80	53380	0.06604	0.193	6.41E-06	0.002832	-11.95762099	
90	19500	0.06604	0.193	1.75E-05	0.002754	-10.95059931	

Table S15. Calculation of ionic conductivity and activation energy of PCN-56 38.4 wt% [NEt_4][TFSI].

Temperature (°C)	Resistance (Ohms)	Thickness (cm)	Area (cm^2)	Conductivity (S/cm)	1/T (K^{-1})	ln (Conductivity)	Activation Energy (eV)
22	19920000	0.07366	0.193	1.92E-08	0.003388	-17.77046509	0.93
40	2385000	0.07366	0.193	1.60E-07	0.003193	-15.64793996	
60	331700	0.07366	0.193	1.15E-06	0.003002	-13.6752165	
70	115800	0.07366	0.193	3.30E-06	0.002914	-12.62285012	
80	47940	0.07366	0.193	7.96E-06	0.002832	-11.74093579	
90	20390	0.07366	0.193	1.87E-05	0.002754	-10.88603014	

Table S16. Calculation of ionic conductivity and activation energy of PCN-56 42.8 wt% [NEt_4][TFSI].

Temperature (°C)	Resistance (Ohms)	Thickness (cm)	Area (cm^2)	Conductivity (S/cm)	1/T (K^{-1})	ln (Conductivity)	Activation Energy (eV)
22	3308000	0.0889	0.193	1.39E-07	0.003388	-15.7870323	0.76
40	776000	0.0889	0.193	5.94E-07	0.003193	-14.3370858	
60	296200	0.0889	0.193	1.56E-06	0.003002	-13.3739682	
70	59500	0.0889	0.193	7.74E-06	0.002914	-11.7689096	
80	26000	0.0889	0.193	1.77E-05	0.002832	-10.9410298	
90	12150	0.0889	0.193	3.79E-05	0.002754	-10.1802625	

Table S17. Calculation of ionic conductivity and activation energy of PCN-56 46.6 wt% [NEt_4][TFSI].

Temperature (°C)	Resistance (Ohms)	Thickness (cm)	Area (cm^2)	Conductivity (S/cm)	1/T (K^{-1})	ln (Conductivity)	Activation Energy (eV)
22	5025000	0.09144	0.193	9.43E-08	0.003388	-16.17694318	0.88
40	689700	0.09144	0.193	6.87E-07	0.003193	-14.19101917	
60	116800	0.09144	0.193	4.06E-06	0.003002	-12.41522552	
70	53010	0.09144	0.193	8.94E-06	0.002914	-11.62524302	
80	19690	0.09144	0.193	2.41E-05	0.002832	-10.63487334	
90	6118	0.09144	0.193	7.74E-05	0.002754	-9.465997694	

Table S18. Calculation of ionic conductivity and activation energy of PCN-56 50 wt% [NEt_4][TFSI].

Temperature (°C)	Resistance (Ohms)	Thickness (cm)	Area (cm^2)	Conductivity (S/cm)	1/T (K^{-1})	ln (Conductivity)	Activation Energy (eV)
22	14840000	0.08636	0.193	3.02E-08	0.003388	-17.31700238	0.88
40	1850000	0.08636	0.193	2.42E-07	0.003193	-15.23486178	
60	285900	0.08636	0.193	1.57E-06	0.003002	-13.36756296	
70	142300	0.08636	0.193	3.14E-06	0.002914	-12.66985837	
80	58720	0.08636	0.193	7.62E-06	0.002832	-11.78470125	
90	16080	0.08636	0.193	2.78E-05	0.002754	-10.48949713	

Table S19. Calculation of ionic conductivity of PCN-56 53.2 wt% [NEt_4][TFSI] at different temperatures.

Temperature (°C)	Resistance (Ohms)	Thickness (cm)	Area (cm^2)	Conductivity (S/cm)	1/T (K^{-1})	ln (Conductivity)	Activation Energy (eV)
22	3050000	0.08382	0.193	1.42E-07	0.003388	-15.76467069	0.82
40	511200	0.08382	0.193	8.50E-07	0.003193	-13.97853473	
60	85360	0.08382	0.193	5.09E-06	0.003002	-12.18865143	
70	43660	0.08382	0.193	9.95E-06	0.002914	-11.51820618	
80	16950	0.08382	0.193	2.56E-05	0.002832	-10.57204166	
90	5683	0.08382	0.193	7.64E-05	0.002754	-9.479253088	

Table S20. Calculation of ionic conductivity and activation energy of PCN-56 57.08 wt% [NEt_4][TFSI].

Temperature (°C)	Resistance (Ohms)	Thickness (cm)	Area (cm^2)	Conductivity (S/cm)	1/T (K^{-1})	ln (Conductivity)	Activation Energy (eV)
22	8744000	0.08636	0.193	5.12E-08	0.003388	-16.78804389	0.97
40	956200	0.08636	0.193	4.68E-07	0.003193	-14.57488796	
60	123400	0.08636	0.193	3.63E-06	0.003002	-12.52735197	
70	45980	0.08636	0.193	9.73E-06	0.002914	-11.54012738	
80	11680	0.08636	0.193	3.83E-05	0.002832	-10.16979884	
90	8059	0.08636	0.193	5.55E-05	0.002754	-9.798710342	

SI 9. References

1) Katz, M. J.; Brown, Z. J.; Colón, Y. J.; Siu, P. W.; Scheidt, K. A.; Snurr, R. Q.; Hupp, J. T.; Farha, O. K. Chem. Commun. 2013, 49 (82), 9449–9451.

2) Jiang, H.-L.; Feng, D.; Liu, T.-F.; Li, J.-R.; Zhou, H.-C. J. Am. Chem. Soc. 2012, 134 (36), 14690–14693.

3). Henderson, W. A.; Seo, D. M.; Zhou, Q.; Boyle, P. D.; Shin, J.-H.; Long, H. C. D.; Trulove, P. C.; Passerini, S. Adv. Energy Mater., 2012, 2, 1343–1350.